# Hierarchy of DNA Damage Recognition in *Escherichia coli* Nucleotide Excision Repair†

Yue Zou,*,‡ Charlie Luo,‡ and Nicholas E. Geacintov#

*Sealy Center for Molecular Science and Department of Human Biological Chemistry & Genetics, University of Texas Medical Branch, Galveston, Texas 77555, and Department of Chemistry, New York University, New York, New York 10003-5180*

*Received June 30, 2000; Revised Manuscript Received January 10, 2001*

ABSTRACT: DNA damage recognition plays a central role in nucleotide excision repair (NER). Here we present evidence that in *Escherichia coli* NER, DNA damage is recognized through at least two separate but successive steps, with the first focused on distortions from the normal structure of the DNA double helix (initial recognition) and the second specifically recognizing the type of DNA base modifications (second recognition), after an initial local separation of the DNA strands. DNA substrates containing stereoisomeric (+)- or (−)-*trans*- or (+)- or (−)-*cis*-BPDE-$N^2$-dG lesions in DNA duplexes of known conformations were incised by UvrABC nuclease with efficiencies varying by up to 3-fold. However, these stereoisomeric adducts, when positioned in an opened, single-stranded DNA region, were all incised with similar efficiencies and with enhanced rates (by factors of 1.4−6). These bubble substrates were also equally and efficiently incised by UvrBC nuclease without UvrA. Furthermore, removal of the Watson−Crick partner cytosine residue (leaving an abasic site) in the complementary strand opposite a (+)-*cis*-BPDE-$N^2$-dG lesion led to a significant reduction in both the binding of UvrA and the incision efficiency of UvrABC by a factor of 5. These data suggest that *E. coli* NER features a dynamic two-stage recognition mechanism.

The most remarkable aspect of nucleotide excision repair (NER)[1] is its ability to remove a large variety of DNA lesions which are structurally and chemically distinct. Examples of these lesions include the major UV-induced photoproducts, the adducts induced by some therapeutic drugs such as cisplatin, and the binding to DNA of metabolites of environmental carcinogens such as polycyclic aromatic hydrocarbons and other chemical agents (*1*−*4*). Such a broad repertoire of substrates, which differ dramatically from that of other enzymatic DNA repair pathways, is the direct result of DNA damage recognition. DNA damage recognition forms the basis for NER in executing its specific function to maintain the genomic integrity in cells. It is widely believed that the successful DNA repair directly depends on the efficient recognition of DNA damage.

Recent studies on both *Escherichia coli* and human NER systems suggest that DNA damage, with and only with concurrent duplex disruption and chemical alteration to nucleotides, can be efficiently recognized and removed by NER enzymes (*3*, *5*−*14*). This has been called bipartite substrate discrimination by Hess et al. (*8*). It remains unclear, however, how these structural and chemical determinants of DNA damage are processed during the recognition. Specifically, little is known about the mechanistic steps involved in the recognition, or how the multiple steps of recognition are organized and coordinated with one another to maximize recognition. Determination of these aspects is crucial for understanding the molecular and mechanistic details of DNA damage recognition and repair in terms of the unique properties of NER. In *E. coli* NER, the UvrABC system carries out the damage recognition and incision steps. Because of its relative simplicity and the general mechanistic similarities between the *E. coli* and eukaryotic NERs, this system has been widely studied as a paradigm for reaching a better understanding of the mechanism of NER.

The enzymatic action of the UvrABC system begins with the dimerization of UvrA. The $UvrA_2$ dimer interacts with UvrB to form a $UvrA_2B$ complex, which then binds to the damaged site (*15*, *16*). Our recent studies indicate that upon binding, the local DNA around the damaged site is unwound by the helicase activity of $UvrA_2B$ (*12*). Our results further suggest that this strand opening leads to the dissociation of $UvrA_2$ and the formation of a stable UvrB-DNA complex (*17*, *18*). The UvrC is then recruited by interaction with the UvrB (*19*) and results in the formation of the UvrBC-DNA pre-incision intermediate containing a bubble-like structure with a size of, for example, 6 bases with 2 unpaired bases 5′ and 3 unpaired bases 3′ to a benzo[*a*]pyrenediol epoxide (BPDE)-DNA lesion (*12*). Formation of this structure-specific intermediate is believed to trigger 3′- and 5′-endonuclease activities in UvrBC, which cleave the phos-

† This study was supported by grants from NIEHS (ES07955 and CA20851).

* All correspondence should be sent to: Yue Zou, Sealy Center for Molecular Science, J-1071, 5th floor MRB, University of Texas Medical Branch, Galveston, TX 77555-1071. Phone: (409)772-2144. Fax: (409)772-1790. E-mail: yzou@utmb.edu.

‡ University of Texas Medical Branch.

# New York University.

[1] Abbreviations: BPDE, benzo[*a*]pyrenediol epoxide, 7,8-dihydroxy-9,10-epoxy-7,8,9,10-tetrahydrobenzo[*a*]pyrene; NP, 1-nitropyrene; DTT, dithiothreitol; EDTA, ethylenediaminetetraacetic acid; NER, nucleotide excision repair; TBE, tris borate EDTA, pH 8.0.

10.1021/bi001504c CCC: $20.00 © 2001 American Chemical Society
Published on Web 02/10/2001

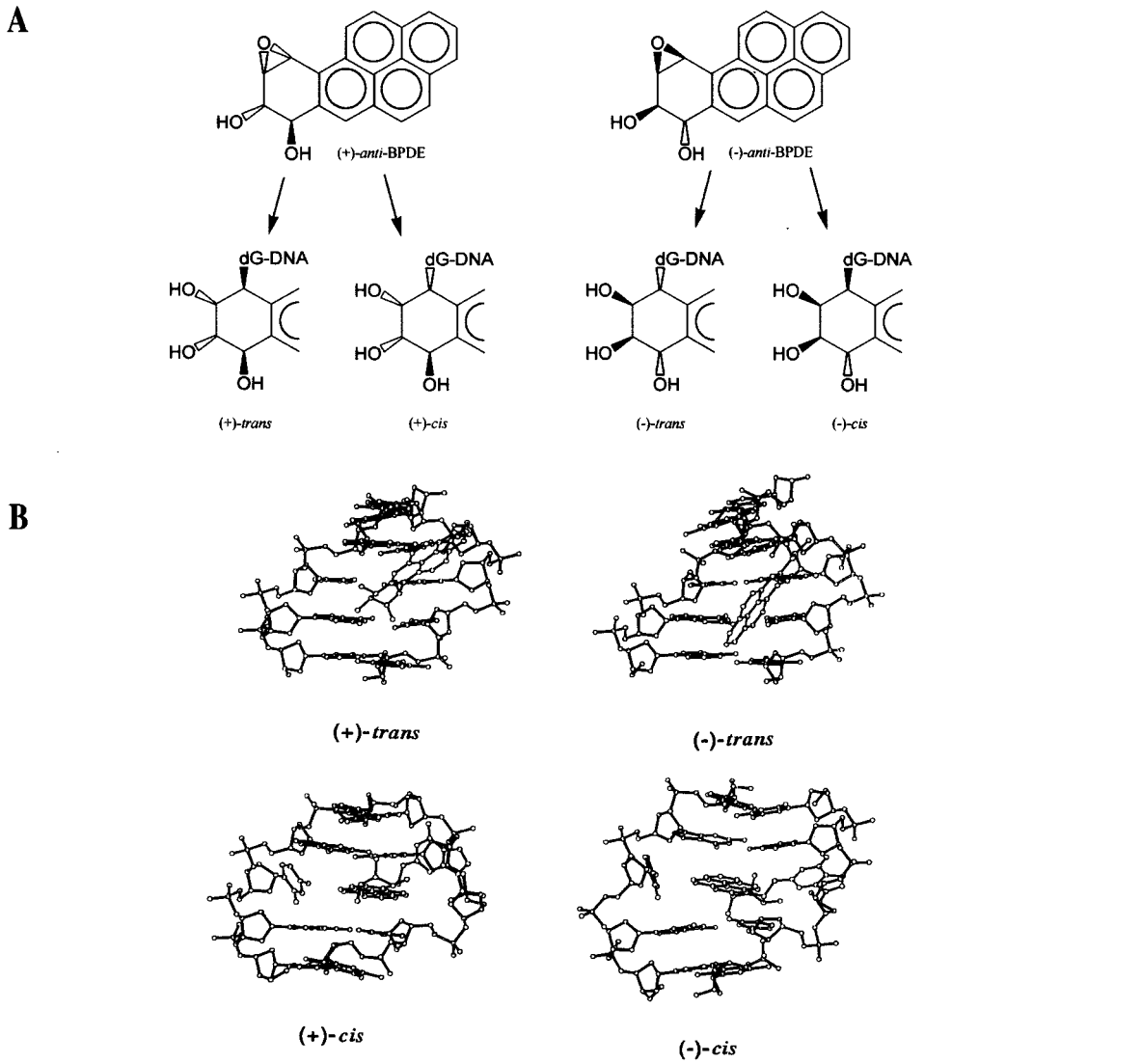


FIGURE 1: DNA adducts and substrates used in the present study: (A) chemical structures of (+)-*trans*-, (−)-*trans*-, (+)-*cis*-, and (+)-*cis*-BPDE-$N^2$-dG DNA adducts; (B) NMR structures of these adducts (*31*−*34*); (C) substrates constructed for this study.

phodiester bonds 4−7 phosphates 3′ and 8 phosphates 5′ to the damaged residue, respectively (*5*, *12*, *20*, *21*).

Benzo[*a*]pyrene (BP), one of the most ubiquitous environmental carcinogens (*22*−*26*), is metabolically activated to the highly reactive and mutagenic diol epoxide BPDE. The latter reacts with DNA primarily at $N^2$-guanine to form an array of stereoisomeric adducts. Specifically, four different stereoisomeric adducts are formed when *anti*-BPDE binds covalently to $N^2$ of guanine (Figure 1). Although these lesions are identical in all respects except for the absolute configurations of the substituents about the chiral carbon atoms, they exhibit striking differences in mutagenic activities (*27*, *28*). Repair studies of these lesions by Zou et al. (*5*) and Hess et al. (*9*) indicate that the rates of incision are strongly dependent on the strikingly different conformational properties of these stereoisomeric adducts. It has been suggested that the observed differential repair rates are probably due to the varying degrees of helical distortions induced by these lesions (Figure 1B) (*5*). These stereoisomeric lesions, therefore, can serve as a structural tool not only for exploring the mechanism of DNA damage processing by NER but also to provide insights into the potential impact of these lesions on mutagenesis.

Our previous studies on strand opening in DNA damage recognition (*12*) led to the hypothesis that DNA damage recognition in NER consists of a series of integrated steps,

each of which may have its own specificity for the structural or chemical characteristics of an adduct. In the present study, we tested this hypothesis and determined the specificity of damage recognition in each step by placing the BPDE-DNA stereoisomeric adducts into structure-specific DNA regions in the substrates. With these structure-specific substrates, the individual steps of damage recognition were examined separately. We demonstrate that the damage recognition in *E. coli* NER is achieved through at least two sequential steps in a process involving DNA strand opening. These two steps sense the distortions in the Watson−Crick duplex and the alteration of chemical integrity of the DNA, respectively. The second step of recognition fully depends on the success of the first one. Furthermore, our results show that the differential repair of the various BPDE-DNA adducts, which may lead to their differences in mutagenesis from translesion synthesis, is due to the different degrees of the duplex distortions induced by these adducts. These distortions are probed during the initial recognition step.

## EXPERIMENTAL PROCEDURES

*Protein Purification.* UvrA was purified from *E. coli* strain MH1 ΔUvrA containing the overproducing plasmid, pSST10 (graciously supplied by L. Grossman, Johns Hopkins University), in which the *uvrA* gene is under the control of the heat-inducible PL promoter. UvrB was purified in one step through a chitin column from *E. coli* strain XL-1 Blue transformed with the overexpressing plasmid pUTG97 containing the *uvrB* gene under the control of the IPTG-induced $P_{tac}$ promoter as described previously (*12*). UvrC was overproduced from *E. coli* C41(DE3) cells (*29*) harboring plasmid pUTG98 containing the PCR-amplified *uvrC* gene, which was subcloned via *Nde*I and *Kpn*I restriction sites into the vector pTYB1 (IMPACT T7 system, New England Biolabs). The entire sequence of *uvrC* was verified after subcloning. Expression of the *uvrC* gene was under the control of the IPTG-induced T7 promotor. The UvrC protein was purified on a chitin column in one step following the same procedures as described previously for UvrB (*12*) except that 500 mM (rather than 100 mM) NaCl was used in the cleavage and elution buffers.

*DNA Substrate Construction.* The 50-bp oligonucleotides containing a single BPDE adduct, (+)- or (−)-*cis*-*anti*-BPDE, (+)- or (−)-*trans*-*anti*-BPDE, or 1-nitropyrene (NP) (graciously supplied by A. Basu, University of Connecticut), were prepared as described previously (*12*). Briefly, the phosphorylated BPDE 11mers (30 pmol), prepared by the methods described by Pirogov et al. (*30*), were ligated with stoichiometric quantities of 20mer and phosphorylated 19mer, using T4 DNA ligase in the presence of a 55mer template strand containing the complementary sequence of 50 bases in a 30-μL solution containing 50 mM Tris-HCl, pH 7.8, 10 mM $MgCl_2$, 10 mM DTT, 1 mM ATP, and 50 μg/mL BSA. The ligation was carried out at 16 °C for 12 h. After ligation, the products were purified and then reannealed with various 50mer template strands to make appropriate substrates, as shown in Figure 1. The annealed substrates were purified on a nondenaturing 8% polyacrylamide gel. The double-stranded character and homogeneity of the 50-bp substrates were examined by a restriction assay (*5*) and analyzed on a 12% polyacrylamide sequencing gel under denaturing conditions with TBE as the running buffer (50 mM Tris-HCl, 50 mM boric acid, 1 mM EDTA, pH 8.0).

The 50-bp oligonucleotides containing a single abasic site opposite a (+)-*cis*-BPDE adduct were constructed by annealing a BPDE-DNA 50mer with a complementary 50mer oligonucleotides containing an abasic site. The abasic site-containing complementary strand was synthesized on an Applied BioSystems 394 DNA/RNA synthesizer by incorporating a dSpace CE phosphoramidite (Glen Research) into the proper site in the DNA sequence.

*Gel Mobility Shift Assays.* Binding of the DNA substrates by the Uvr proteins was determined by gel mobility shift assays. Typically, the substrate (3 nM) was incubated with UvrA (10 nM) and/or UvrB (250 nM) and/or UvrC (50 nM) at 37 °C for the period indicated in the figure legends in 20 μL of UvrABC buffer (50 mM Tris-HCl, pH 7.5, 50 mM KCl, 10 mM $MgCl_2$, 5 mM DTT) in the presence or absence of 1 mM ATP. After incubation, 2 μL of 80% (v/v) glycerol was added and the mixture was immediately loaded onto a 3.5% native polyacrylamide gel in TBE running buffer and electrophoresed at room temperature. For the binding studies with proteins other than UvrA, ATP (1 mM) and $MgCl_2$ (10 mM) were present in the TBE running buffer.

*Incision Assays.* The 5′-terminally labeled DNA substrates (3 nM) were incised by UvrABC or UvrBC (UvrA, 10 nM; UvrB, 250 nM; UvrC, 50 nM) in the UvrABC buffer (1 mM ATP) at 37 °C for 15 or 30 min. For the incision kinetics measurement, the substrates were incised for 0, 5, 10, and 15 min. The Uvr subunits were diluted and premixed into storage buffer before mixing with DNA. The reactions were terminated by adding EDTA (20 mM) or heating to 90 °C for 3 min. The samples were denatured with formamide and heated to 90 °C for 5 min and then quick-chilled on ice. The digested products were analyzed by electrophoresis on a 12% polyacrylamide sequencing gel under denaturing conditions with TBE buffer.

## RESULTS

*Damage Recognition and Incision in an Opened DNA Structure.* The construction of the substrates used in this study followed the procedures described previously (*5, 12*) and are shown in Figure 1C. These 50-bp substrates contain a single DNA adduct with either (+)- or (−)-*trans*- or (+)- or (−)-*cis*-BPDE-$N^2$-dG (Figure 1A) or NP in the center of the upper strand, as depicted. The structures of these lesions in normal double-stranded DNA have been established by NMR methods (Figure 1B). Briefly, the aromatic pyrenyl residues of (+)- and (−)-*trans*-$N^2$-dG lesions lie in the minor grooves pointing in the 5′- and 3′-directions of the modified strands, respectively (*31, 32*). In contrast, the pyrenyl residues of the (+)- and (−)-*cis*-adducts intercalate into the helix with the modified guanine and partner cytosine bases displaced into the minor and major grooves, respectively (*33, 34*). The NP-C8-dG adduct also assumes an intercalative base displacement conformation in which the pyrenyl residue stacks with the neighboring bases while the modified guanine and partner cytosine bases are displaced into or toward the major groove (*35*). The bubble substrates (BS) in Figure 1C used in this study are featured with a DNA structure containing 6 mismatched bases, with 2 bases 5′ and 3 bases 3′ to the adduct. This defined bubble structure is used to mimic the

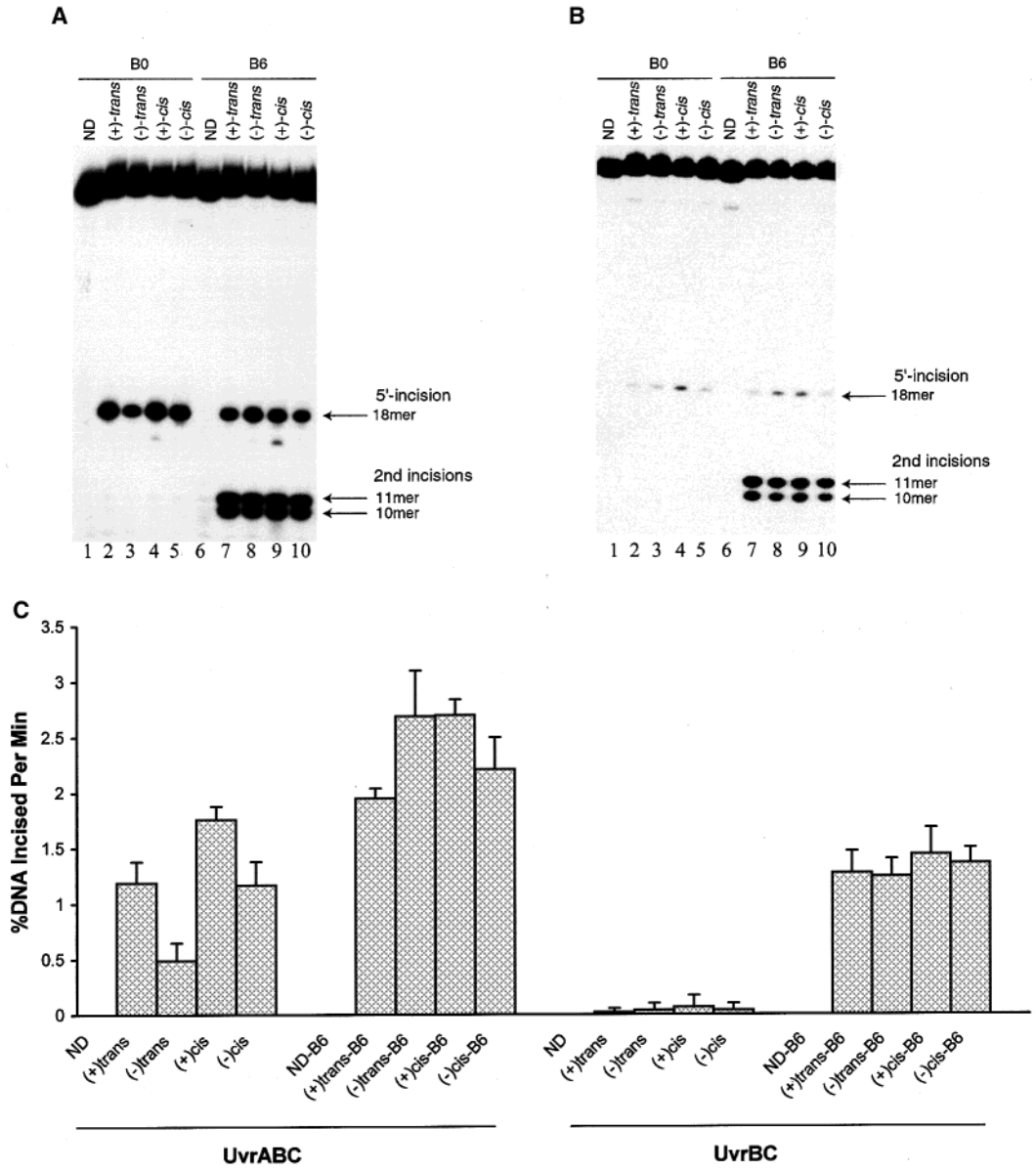


FIGURE 2: Incision of BPDE-DNA bubble substrates by UvrABC (A) and UvrBC (B) as compared with the normal, nonbubble DNA duplex substrates. The 5′-terminally labeled DNA substrates containing a BPDE adduct in a 6-base open structure or a normal structure were incubated with UvrABC (UvrA, 10 nM; UvrB, 250 nM; UvrC, 50 nM) (A) or UvrBC in the absence of UvrA (B), in the UvrABC buffer at 37 °C in a time-course manner. The incision products were then analyzed on 12% polyacrylamide sequencing gels and quantified (C) using PhosphorImager (Molecular Dynamics). The incision rates were then determined. The data represent the means ± SD (the standard deviation that is derived from at least three independent experiments). ND stands for nondamaged DNA.

DNA strand opening formed in the recognition and repair intermediates during the interaction of UvrABC with the BPDE-DNA adduct (*12*). Such an open conformation was also found to be true for the NP-DNA adduct (data not shown). In the single-stranded region of the bubble, the differences in adduct-induced helical distortion observed in DNA duplex should become irrelevant. Thus, by using these structure-specific substrates, individual steps of damage recognition can be examined separately.

DNA strand opening around an adduct is a dynamic process that is required for efficient damage recognition and repair (*12*). To further explore the mechanistic details and to determine the specificity of the individual steps of DNA damage recognition in NER, the DNA substrates containing the four BPDE stereoisomeric adducts in bubble or nonbubble structures were incised by UvrBC nuclease in the presence or absence of UvrA (Figure 2A,B). The data were quantified as shown in Figure 2C. As shown in Figure 2A,B, besides the normal 5′-incision, additional incisions (the second incisions) were observed with the bubble substrates. These incisions occurred at the 15th and 16th phosphodiester bonds 5′ to the adduct or the seventh and eighth phosphodiester bonds 5′ to the normal 5′-incison site. Moolenaar et al. (*36*) and Gordienko and Rupp (*37*) have recently reported a new type of damage-independent nuclease activity of UvrABC or UvrBC making incisions at the seventh and eighth phosphodiester bonds 5′ to a double-stranded DNA nicked site. Since the normal 5′-incision produces a similar DNA structure required for the incisions by the damage-independent nuclease activity of UvrBC, the second incisions observed here may result from this same nuclease activity. However, it seems unlikely that two different UvrB/UvrBC-DNA complexes can form simultaneously on the same 50-bp DNA molecule at such a close distance and independently

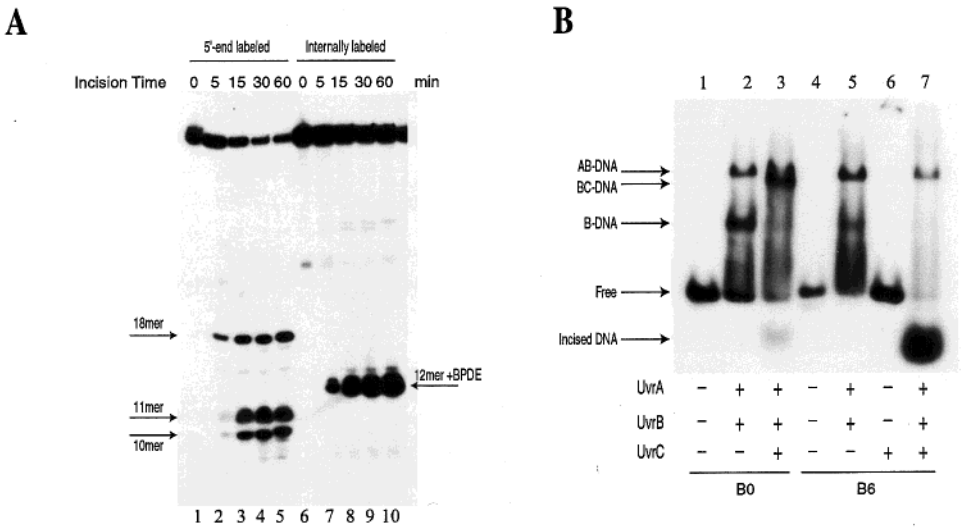


FIGURE 3: Characterization of the second 5′-incisions of the bubble substrates (B6) produced by UvrABC or UvrBC. (A) The internally labeled (+)-*cis*-BPDE-DNA bubble substrate was incised by UvrABC (UvrA, 10 nM; UvrB, 250 nM; UvrC, 50 nM) at 37 °C for the indicated periods in comparison with the same substrate labeled at the 5′-end. The 18mer is the 5′-incision product, and the 10mer and 11mer are the second 5′-incision products. (B) Binding of UvrA, UvrB, and UvrC subunits to the bubbled and nonbubbled (+)-*cis*-BPDE-DNA substrates. Substrates were incubated with Uvr proteins in the UvrABC buffer at 37 °C for 45 min and then subjected to analysis on a 3.5% native polyacrylamide gel with 10 mM $MgCl_2$ and 1 mM ATP in both the gel and running buffer. AB-DNA, BC-DNA, and B-DNA represent UvrAB-DNA, UvrBC-DNA, and UvrB-DNA complexes, respectively.

produce the two types of 5′-incisions. Therefore, the UvrBC should dissociate from the bubbled DNA after the normal dual incisions of adduct to make the nicked site accessible to the UvrBC complex for the second 5′-incisions (coupled-exclusive mode). To confirm this mechanism, experiments were performed as shown in Figure 3. In Figure 3A, the DNA bubble substrates (B6) were internally labeled at the sixth phosphate 5′ to the adduct and then subjected to incision by UvrABC. The results were compared to those obtained with a normally 5′-end-labeled bubble substrate (Figure 3A). The observation of a single BPDE-adducted 12mer as the incision product for the internally labeled substrate strongly suggests that the second incisions are coupled with the normal 5′-incision. Otherwise, additional bands for the 39mer and 40mer representing the second incisions without the normal 5′-incision would have been observed. This result is consistent with the observation reported by Visse et al. (*38*) although there nonbubbled DNA substrate was used. The possible dissociation of UvrBC from the DNA after the normal dual incisions was examined in the gel mobility shift assay as shown in Figure 3B. For the normal duplex substrate (B0), the UvrBC remains a stable complex with DNA even after the dual incisions, as indicated by a separate band migrating barely faster than the one for UvrAB-DNA complex (lane 3, Figure 3B). This is consistent with the previous results reported by Van Houten et al. (*39*). In contrast, the UvrBC fails to remain as a complex with the DNA by releasing the incised DNA fragment in the case of the bubble substrate (lane 7, Figure 3B), indicating that UvrBC dissociates from the DNA after the incisions. Taken together, our results indicate that the damage-independent nuclease activity of UvrBC is responsible for the second incisions observed with the bubble substrates, and the incisions occur by coupling with the damage-dependent 5′-incision. The occurrence of the second incisions makes the first incisions become invisible in the gel. Therefore, the actual efficiency of the damage-specific 5′-incision is determined by combining the bands in the gel for both the 5′- and second incisions (Figure 2).

Figure 2C shows the quantification of the UvrABC and UvrBC incisions of the four BPDE-DNA stereoisomeric adducts either in the normal DNA duplex or in an opened DNA structure. For the normal DNA substrates, these adducts are incised by UvrABC with significantly different efficiencies, especially between (+)-*cis*- and (−)-*trans*-BPDE-DNA. However, these differences seem to be dramatically reduced or eliminated as these adducts are placed in a bubble structure (Figure 2C). The same results were also observed for the incisions in the absence of UvrA (Figure 2C). Analysis of the incision rate for each BPDE-DNA stereoisomer by an independent Student's *t*-test indicated that the UvrABC incisions of the nonbubble substrates (B0), (+)-*trans*- versus (−)-*trans*-, (+)-*trans*- versus (+)-*cis*-, and (−)-*trans*- versus (+)-*cis*-BPDE-DNA, are significantly different, with *P* vaules of 0.025, 0.0011, and 0.0012, respectively, whereas the difference between (−)-*trans* and (−)-*cis* is of borderline significance ($P = 0.066$). In contrast, no comparison between the bubble substrates (B6) has been found to be significantly different, except the (+)-*trans* versus (+)-cis which has a *P* value of 0.011. Similarly, the UvrBC incisions (in the absence of UvrA) of these stereoisomeric bubble substrates have no significant difference at all.

*Recognition of Distorted DNA Structures.* The results presented above implicate an initial damage recognition mechanism in *E. coli* NER that occurs prior to strand opening. Recent studies on damage recognition suggest that distortions in the normal DNA duplex structure are recognized by repair proteins (*3, 5, 7*−*12*). It is, therefore, reasonable to suggest that this initial level of recognition may primarily sense the disruption of Watson−Crick base pairing induced by various kinds of DNA damage. To examine this issue, experiments were conducted as shown in Figure 4. In this experiment, DNA substrates of 50 bp containing a (+)-*cis*-BPDE-modified guanine opposite either an abasic pyrim-

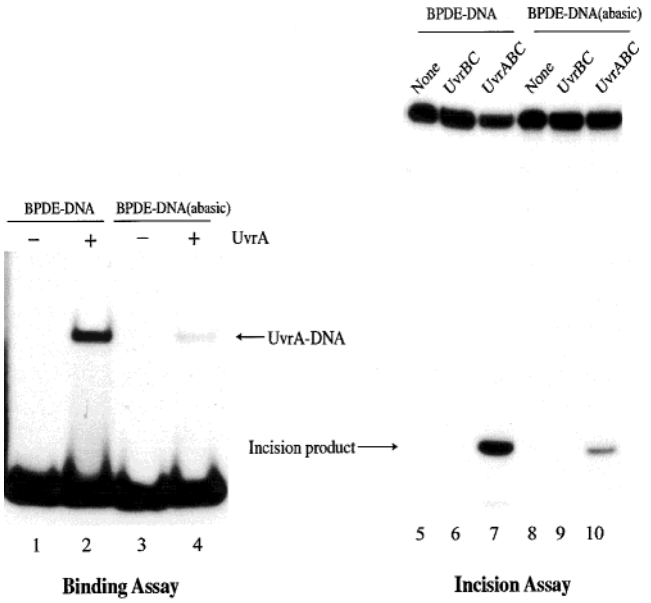


FIGURE 4: Incision and binding of DNA substrate containing an abasic residue opposite the BPDE-modified nucleotide by Uvr proteins. The incision was carried out in the UvrABC buffer at 37 °C for 30 min and analyzed on a 12% polyacrylamide sequencing gel. The binding assay was performed with UvrA (10 nM) in the UvrABC buffer in the absence of ATP at 37 °C for 15 min and then analyzed on a 3.5% native polyacrylamide gel with TBE running buffer.

idine (AP) residue or a cytosine in the complementary strand were constructed and then subjected to UvrA binding and UvrABC incision. NMR structural analysis of the (+)-*cis*-BPDE-dG adduct in the same DNA sequence context revealed that the (+)-*cis*-BPDE residue intercalates between DNA bases by rupturing the modified guanine−cytosine base pair and by displacing the modified guanine and cytosine residues into the minor and major grooves, respectively (*33*; also see Figure 1C). The displacement of the guanine and cytosine bases by BPDE results in a significant helical distortion in the DNA structure. Therefore, removal of the cytosine base opposite the modified guanine in the duplex should substantially reduce the extent of DNA distortion induced by the adduct. As shown in Figure 4, both the $UvrA_2$ binding (lane 4) and thus the UvrABC incision (lane 10) dramatically decreased as the cytosine base opposite the BPDE-modified guanine is deleted (abasic DNA substrate). The difference in both the binding and incision efficiency of the (+)-*cis*-BPDE-DNA normal duplex (lanes 2 and 7) and the (+)-*cis*-BPDE-(abasic) substrate (lanes 4 and 10) is about 5-fold. It is interesting to note that the absence of the cytosine base caused a significant decrease in the binding and incision rather than an increase which might have been expected for an enhancement in DNA damage such as the creation of an abasic site. The good correlation between the binding and incision suggests that the binding efficiency was directly responsible for the overall incision efficiency in this case. In contrast, the difference in incision efficiency between the (+)-*cis*-BPDE-dG and (+)-*cis*-BPDE-dG(abasic) adducts in the bubble substrates (B6) was small (data not shown). Apparently, these two adducts are processed with roughly equal efficiencies during the second recognition. Similar results were also obtained in a study of the incision of intrastrand DNA cross-links by a set of carbon tethers which

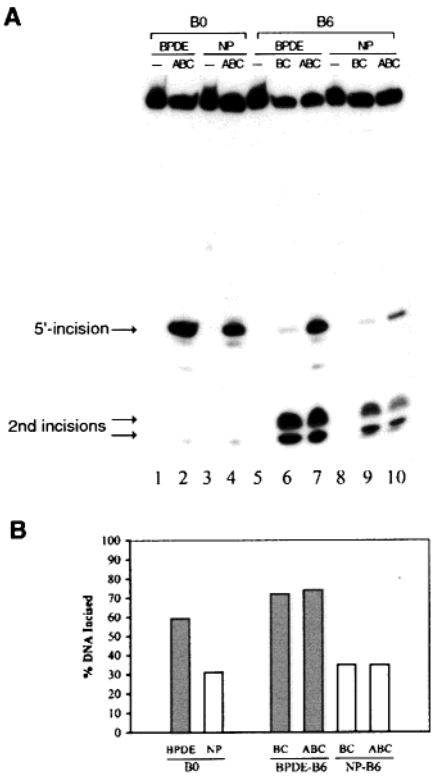


FIGURE 5: UvrABC incision comparison between the (+)-*cis*-BPDE-DNA and NP-DNA adducts in bubble or nonbubble substrates. The incisions were carried out in the UvrABC buffer at 37 °C for 30 min, analyzed on a 12% polyacrylamide sequencing gel (A), and then quantified using PhosphorImager (B). BC stands for UvrBC and ABC for UvrABC.

produce different degrees of DNA bending around the adduct (*40*). In this study, the ability of UvrABC nuclease to recognize and incise the adducts was inversely dependent on the length of the $N^2-N^2$ guanine carbon linkers which inversely correlates with the extent of the DNA bending. All of these results suggest that the lesion-induced helical distortions are the major determinants for the initial recognition and indeed recognized predominantly at this first step.

*Recognition and Incision of BPDE- and NP-DNA Adducts.* To further explore and confirm the properties of damage recognition that follow strand opening in a normal duplex, adducts with different types of chemical modifications to a dG residue positioned in the bubble structure were compared for recognition and incision by UvrABC. As shown in Figure 5, the UvrABC nuclease incises the (+)-*cis*-BPDE-$N^2$-dG adduct about 2-fold more efficiently than an NP-C8-dG adduct, in both the normal (B0) and bubble (B6) substrates. The results of the bubble substrates imply that the second recognition step does distinguish between chemically different types of base modification, although it is unable to distinguish between stereoisomeric BPDE-$N^2$-dG adducts (Figure 2). Furthermore, the incision efficiencies of these two adducts in the opened DNA structure (B6) are only slightly higher than those of the nonbubble substrate (B0), suggesting that the helical distortions associated with these two adducts are similar. This is consistent with fact that both the (+)-*cis*-BPDE-$N^2$-dG and NP-C8-dG adducts exhibit base-displaced intercalated conformations (*33*, *35*) which can be efficiently and probably equally recognized by $UvrA_2B$

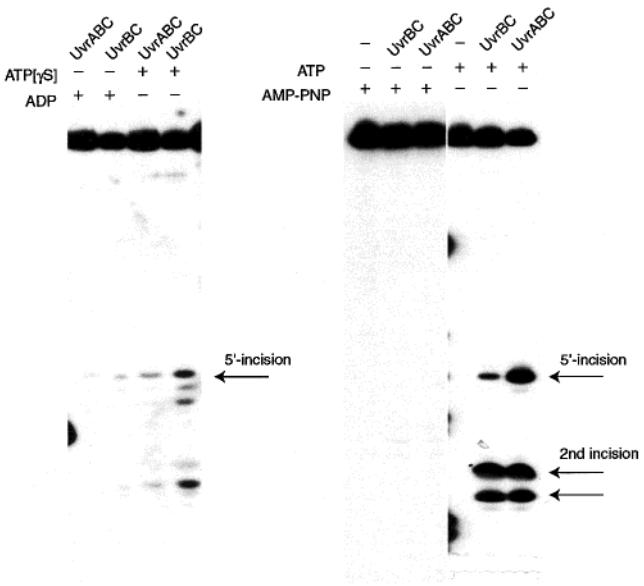


FIGURE 6: Incision of (+)-*cis*-BPDE-DNA bubble substrates (B6) by Uvr proteins in the presence of ATP or its analogues. The incision was carried out in the UvrABC buffer in the presence of ATP or its analogues at 37 °C for 30 min. The incision products were analyzed on a 12% polyacrylamide sequencing gel.

at the initial step. These results confirm that the differences of incision efficiency between the (+)-*cis*-BPDE and NP adducts can be attributed to damage recognition after strand opening.

*ATP Hydrolysis in Damage Recognition and Incision.* Since ATP plays an important role in DNA damage recognition and incision by UvrABC, experiments were performed with ATP and its analogues to determine whether ATP binding or hydrolysis is required for the incisions of the intermediate-like bubble substrates by UvrBC nuclease in the presence or absence of UvrA. As shown in Figure 6, the substitution of ATP with ATP($\gamma$S) dramatically lowers the incision efficiency, suggesting that the ATP binding itself may not be sufficient to cause an efficient incision by UvrABC. Interestingly, the UvrBC nuclease incises the substrate much more efficiently in the absence of UvrA than in its presence. This is likely because the UvrA by itself can bind specifically to DNA lesions in the absence of ATP and thus inhibits the access of UvrBC to the same lesion. In this case, the $UvrA_2B$ complex does not form since ATP is required for its formation (*1*). In the presence of ATP, the hydrolysis of ATP results in dissociation of the UvrA dimer (*41*) so that the UvrBC binding is not affected at the low concentrations of UvrA used in that study. In the presence of ATP($\gamma$S), the hydrolysis of ATP($\gamma$S) is greatly reduced as compared with ATP, and therefore, dissociation of the UvrA dimer from the damage site is inhibited. In comparison to ATP($\gamma$S), little or no incision was observed in the presence of ADP (a hydrolyzed product of ATP) or AMP-PNP, respectively. We previously reported that ADP could facilitate the 5′-incision of a nondamaged, 3′-nicked Y-shaped substrate by 77%, as compared with ATP, although the incision efficiency was very low (*21*). It is possible that the lack of incision in the presence of ADP may be due to the lack of the 3′-incision. Both ATP($\gamma$S) and ADP were reported to bind to the same sites as ATP does in UvrA (*42*). Most likely, this is also true in the case of UvrB which has an ATP binding site (*1, 43, 44*). All of these facts imply that not only the binding of ATP($\gamma$S) and ADP but also the hydrolysis of ATP are required for incisions, particularly in the case of the 3′-incision.

## DISCUSSION

DNA damage is repaired by NER with varying efficiencies, which is believed to result from different structural and chemical modifications of the DNA associated with different lesions. This differential repair may ultimately lead to different biological consequences. It is clear that DNA damage recognition plays a central role in this process and characterizes this particular repair pathway. Information on how the DNA damage is processed by repair proteins during NER will be very helpful in understanding the overall mechanism of NER. In the present study, we have identified the individual damage recognition steps, examined these steps separately, and determined their specificity for lesions and their impact on NER.

Comparison of the data between the bubbled and nonbubbled substrates in Figure 2 reveals three important observations: (1) the strand opening around the adducts (B6) results in a clear enhancement of incision efficiency, particularly for the (−)-*trans*-BPDE-DNA adduct where a dramatic enhancement occurs; (2) all of the observed differences in incision efficiency between these adducts almost vanish when the strands are separated from one another in the bubbles; and (3) even in the absence of UvrA, UvrBC efficiently incises the bubble substrates without adduct-type bias. These results suggest that two separate steps of damage recognition are involved, one including the UvrA (and UvrB) and the other excluding the UvrA after a strand opening. In this case, the strand separation facilitates the damage recognition by factors of 1.4−6, depending on the stereochemistry of the adducts (Figure 2). In particular, the (−)-*trans*-BPDE-DNA adduct in the nonbubble substrate (B0) is poorly incised, which is most likely due to the poor recognition of this adduct in the initial step. This is because the presence of the bubbles dramatically increases the incision efficiency. The preexisting strand separation with proper structures allows the initial recognition step to be skipped and permits the UvrB/UvrBC to fully access the modified nucleotide which is initially partially buried in the DNA duplex. The elimination of the incision differences among these stereoisomeric adducts in an opened DNA structure (B6), especially between the (+)-*cis*- and (−)-*trans*-BPDE-DNA adducts, further supports these points since all of the adducts are chemically identical except for the absolute configurations of the substituents about the chiral carbon atoms. The stereoisomerically induced differences in helical distortion among these adducts (Figure 1B) can be recognized only in the initial step, but not in the second where the strand opening overrides the effect of helical distortion.

Our results demonstrate that damage recognition is a dynamic, stepwise process that occurs through a series of sequential steps of recognition rather than a simple single binding process. Each of the steps is primarily responsible for recognition of a specific characteristic of a DNA lesion or form of DNA damage and has its own specificity for structural and chemical alterations associated with different lesions. Specifically, *E. coli* NER is initiated by the recogni-

tion of DNA helical distortions by the $UvrA_2B$ protein complex that appears to monitor the stabilization of Watson−Crick base pairs. Upon the success of the initial step, the DNA is unwound around the lesion site. Thus an open structure forms allowing the lesion to be fully accessible to the repair proteins for further recognition of the chemically modified nucleotide, by examination of the chemical integrity of the nucleotide. This mechanism of damage recognition is supported by the observations that (1) $UvrA_2B$ contains helicase activity (*12*, *19*, *45*); (2) DNA adduct in a defined opened DNA structure is efficiently recognized and incised by UvrBC even in the absence of UvrA, while the non-bubbled substrates cannot be incised by UvrBC without UvrA; (3) preexistence of a DNA strand opening around the BPDE adducts enhances the recognition and incision efficiency and eliminates the differences in incision efficiency among these stereoisomeric adducts observed with the normal DNA duplex substrates; (4) relief of the DNA distortion induced by DNA adducts correspondingly reduces the binding by the initial damage recognition protein UvrA and thus diminishes the incision efficiency; and (5) chemically different DNA adducts in an opened DNA structure are recognized and incised with different efficiencies.

Although the two DNA-modifying components, helical distortion and chemical modification, are basically identified separately by the UvrABC system, they are processed in a sequential manner, indicating that the action of the second recognition step depends on the success of the initial one. The final dual incisions are determined by the result of the two levels of recognition. Lacking either of them may result in little or no incision at all.

The study with the substrate containing the BPDE adduct opposite an abasic residue provides some more interesting details on the determinants of DNA damage for the initial discrimination. As indicated by the results, the creation of the abasic site did not result in any increase in damage recognition by the UvrABC system. Instead, a pronounced reduction in both binding and incision due to the removal of the cytosine base in the opposite strand is observed. This suggests that the presence of an abasic residue in the duplex by itself may not be a critical determinant for recognition at the initial step. It is the distortion in the overall structure of the DNA double helix caused by bulky lesions that plays one of the crucial roles in determining the substrate spectrum of *E. coli* NER, making it different from other DNA repair pathways. For example, in normal duplexes the base-displaced (+)-*cis*-BPDE-$N^2$-dG adduct is more readily excised by UvrABC than the minor groove (+)-*trans*-adduct in which Watson−Crick base pairing is intact, with similar observations relevant to the (−)-*trans*- and (−)-*cis*-BPDE-$N^2$-dG lesions (*5*). In the case of excision of the identical lesions by human NER proteins, this *trans/cis* difference is even more pronounced (*9*). However, it should be noted that, since the binding of $UvrA_2$ to the DNA lesions did not fully correlate with the incision efficiency between these BPDE adducts (*6*), the binding of $UvrA_2$ to the adducts may not be the same in all cases as that of $UvrA_2B$ which actually initiates the NER. On the other hand, the two types of binding may be similar, but other minor determinants, in addition to the major distortions of the DNA helix, may also be involved in the initial recognition step.

Our results also suggest that the initial discrimination of the lesion-induced DNA helical distortion is primarily responsible for the differences in incision efficiency among the four stereoisomeric BPDE-DNA adducts. This is consistent with our suggestion that the degree of helical distortion induced by a lesion may primarily determine the overall efficiency of the initial lesion recognition. In other words, the different extent of distortions of the helical DNA duplexes, rather than the nature of the base modifications associated with these stereoisomeric adducts, results in the observed differential incision efficiencies. Results from the present and previous (*5*) studies have shown that the (+)- or (−)-*cis*-adducts are incised more rapidly than the corresponding (+)- or (−)-*trans*-adducts, even though the melting temperature, $T_m$, of 11mer duplexes containing the identical lesions are generally higher in the case of the *cis*- than the *trans*-adducts (*46*). While the *trans*-BPDE adducts are positioned in the minor groove, the *cis*-adducts are intercalated, with the modified guanine and partner cytosine bases displaced out of the helix (for a review, see ref *47*). Apparently, the UvrABC proteins recognize and incise the base-displaced intercalative adducts more readily than the minor groove ones, even though the $T_m$ values of the *cis*-adducts are higher than those of the minor groove *trans*-adducts. The higher $T_m$ values of the *cis*-adducts have been attributed to carcinogen−DNA base-stacking interactions. Therefore, the differences in incision efficiency between these BPDE-DNA adducts reflect the differences in initial recognition of a number of complex conformational factors that determine the degree of helical distortions (such as bending, kinking, and unwinding), rather than only the degree of local DNA denaturation.

Since these adducts are very different in their biological consequences, e.g. mutagenicity (*27*, *28*), the information obtained from this study may help to establish the relationships between the structural nature of the BPDE-DNA damage and the mutagenic potential. It should be noted, however, that the rate of DNA repair is not the sole determinant of the mutagenic potential. Rather, this is likely to depend on the interaction of the particular lesion with whichever polymerase is able to perform translesion synthesis, in addition to the rate of repair. The mutagenic potentials of the four lesions have been studied in site-directed mutagenesis systems (*27*, *28*). It has been reported that in *E. coli*, the (−)-*cis*-adduct has higher miscoding potential dominated by G → T transversions than the (+)-*cis*-adduct and that *cis*-adducts, especially (−)-*cis*-adducts, are consistently more mutagenic than the comparable *trans*-adduct (*28*). Furthermore, the adduct mutagenesis is more dependent on the sterochemistry of the adduct bond than on the stereochemistry of the hydroxyl groups (*27*). However, in these studies, different sequence contexts around the adduct were used than the one in this study. Different DNA sequence contexts may result in different adduct conformations and therefore different repair efficiencies. Although a direct comparison of these mutagenic data with the incision results obtained in the present study seems to be difficult due to the use of different sequence contexts at the adduct, the mutagenic information indicates that the mutagenic potential of these BPDE-DNA adducts strongly depends on the conformational structures of the adducts.

Although the *E. coli* and human NER systems are different regarding the number of proteins participating in the process, as well as the sizes of the damaged DNA patches incised, the two systems share many common mechanistic aspects (*12*). The present study further supports these mechanistic similarities. As with the *E. coli* NER, the DNA damage recognition step in human NER is determined by the bipartite substrate discrimination mechanism in which the concurrence of the disruption of Watson−Crick base pairing and changes in DNA chemistry are required for efficient incision (*8*, *13*). Taken together with the fact that strand opening occurs during human NER (*48*, *49*), this implies that human NER may process DNA damage in a similar way as defined in this study for *E. coli*. Therefore, this damage recognition mechanism may represent one of the most common characteristics of NER.

## ACKNOWLEDGMENT

We thank Drs. R. Stephen Lloyd and Ben Van Houten for their generous support and encouragement. We also thank Dr. Ashis Basu for graciously supplying the NP-adducted DNA 11mer and Dr. David Konkel for the critical reading of this manuscript. The racemic BPDE used in the synthesis of the oligonucleotides was purchased from the National Cancer Institute (NCI/NIH) NCI Chemical Carcinogen Reference Standard Repository.

## REFERENCES

1. Van Houten, B. (1990) *Microbiol. Rev. 54*, 18−51.
2. Wood, R. D. (1996) DNA repair in eukaryotes. *Annu. Rev. Biochem. 65*, 135−67.
3. Wood, R. D. (1999) *Biochimie 81*, 39−44.
4. Sancar, A. (1996) *Annu. Rev. Biochem. 65*, 43−81.
5. Zou, Y., Liu, T. M., Geacintov, N. E., and Van Houten, B. (1995) *Biochemistry 34*, 13582−93.
6. Zou, Y., Bassett, H., Walker, R., Bishop, A., Amin, S., Geacintov, N. E., and Van Houten, B. (1998) *J. Mol. Biol. 281*, 107−19.
7. Lloyd, S., and Van Houten, B. (1995) DNA Damage Recognition. In *DNA Repair Mechanisms: Impact on Human Diseases and Cancer* (Vos, Jean-Michel, Ed.) Chapter 2, pp 25−66, R. G. Landes Co., Biomedical Publishers, Austin, TX.
8. Hess, M. T., Schwitter, U., Petretta, M., Giese, B., and Naegeli, H. (1997) *Proc. Natl. Acad. Sci. U S A. 94*, 6664−9.
9. Hess, M. T., Gunz, D., Luneva, N., Geacintov, N. E., and Naegeli, H. (1997) *Mol. Cell Biol. 17*, 7069−76.
10. Mu, D., Tursun, M., Duckett, D. R., Drummond, J. T., Modrich, P., and Sancar, A. (1997) *Mol. Cell Biol. 17*, 760−9.
11. Moggs, J. G., Szymkowski, D. E., Yamada, M., Karran, P., and Wood, R. D. (1997) *Nucleic Acids Res. 25*, 480−90.
12. Zou, Y., and Van Houten, B. (1999) *EMBO J. 18*, 4889−901.
13. Buschta-Hedayat, N., Buterin, T., Hess, M. T., Missura, M., and Naegeli, H. (1999) *Proc. Natl. Acad. Sci. U.S.A. 96*, 6090−5.
14. Lindahl, T., and Wood, R. D. (1999) *Science 286*, 1897−905.
15. Orren, D. K., and Sancar, A. (1989) *Proc. Natl. Acad. Sci. U.S.A. 86*, 5237−41.
16. Orren, D. K., and Sancar, A. (1990) *J. Biol. Chem. 265*, 15796−803.
17. Oh, E. Y., and Grossman, L. (1986) *Nucleic Acids Res. 14*, 8557−71.
18. Shi, Q., Thresher, R., Sancar, A., and Griffith, J. (1992) *J. Mol. Biol. 226*, 425−32.
19. Lin, J.-J., Phillips, A. M., Hearst, J. E., and Sancar, A. (1992) *J. Biol. Chem. 267*, 17693−700.
20. Lin, J.-J., and Sancar, A. (1992) *J. Biol. Chem. 267*, 17688−92.
21. Zou, Y., Walker, R., Bassett, H., Geacintov, N. E., and Van Houten, B. (1997) *J. Biol. Chem. 272*, 4820−7.
22. Conney, A. H. (1982) *Cancer Res. 42*, 4875−917.
23. Wei, D., Maher, V. M., and McCormick, J. J. (1995) *Proc. Natl. Acad. Sci. U.S.A. 92*, 2204−8.
24. Denissenko, M. F., Pao, A., Tang, M.-S., and Pfeifer, G. P. (1996) *Science 274*, 430−2.
25. Craig, A., Elmets, C. A., Anderson, C. Y., and Mukhtar, H. (1997) *Environmental Toxicology and Pharmacology*, Vol. 4, Issue 3−4, pp 289−93.
26. McGregor, W. G., Wei, D., Chen, R. H., Maher, V. M., and McCormick, J. J. (1997) *Mutat Res. 376*, 143−52.
27. Shukla, R., Jelinsky, S., Liu, T., Geacintov, N. E., and Loechler, E. L. (1997) *Biochemistry 36*, 13263−9.
28. Fernandes, A., Liu, T., Amin, S., Geacintov, N. E., Grollman, A. P., and Moriya, M. (1998) *Biochemistry 37*, 10164−72.
29. Miroux, B., and Walker, J. E. (1996) *J. Mol. Biol. 260*, 289−98.
30. Pirogov, N., Shafirovich, V. Ya., Kolbanovskiy, A., Chen, J., Solntsev, K., Amin, S., and Geacintov, N. E. (1998) *Chem. Res. Toxicol. 11*, 381−8.
31. Cosman, M., de los Santos, C., Fiala, R., Hingerty, B. E., Singh, S. B., Ibanez, V., Margulis, L. A., Live, D., Geacintov, N. E., Broyde, S., and Patel, D. J. (1992) *Proc. Natl. Acad. Sci. U.S.A. 89*, 1914−8.
32. de los Santos, C., Cosman, M., Hingerty, B. E., Ibanez, V., Margulis, L. A., Geacintov, N. E., Broyde, S., and Patel, D. J. (1992) *Biochemistry 31*, 5245−52.
33. Cosman, M., de los Santos, C., Fiala, R., Hingerty, B. E., Ibanez, V., Luna, E., Harvey, R., Geacintov, N. E., Broyde, S., and Patel, D. J. (1993) *Biochemistry 32*, 4145−55.
34. Cosman, M., Hingerty, B. E., Luneva, N., Amin, S., Geacintov, N. E., Broyde, S., and Patel, D. J. (1996) *Biochemistry 35*, 9850−63.
35. Mao, B., Vyas, R. R., Hingerty, B. E., Broyde, S., Basu, A. K., and Patel, D. J. (1996) *Biochemistry 35*, 12659−70.
36. Moolenaar, G. F., Bazuine, M., van Knippenberg, I. C., Visse, R., and Goosen, N. (1998) *J. Biol. Chem. 273*, 34896−903.
37. Gordienko, I., and Rupp, W. D. (1998) *EMBO J. 17*, 626−33.
38. Visse, R., de Ruijter, M., Brouwer, J., Brandsma, J. A., and van de Putte, P. (1991) *J. Biol. Chem. 266*, 7609−17.
39. Van Houten, B., Gamper, H., Hearst, J. E., and Sancar, A. (1988) *J. Biol. Chem. 263*, 16553−60.
40. Kowalczyk, A., Carmical, J. R., Zou, Y., Van Houten, B., Lloyd, R. S., Harris, C. M., and Harris, T. M. (2000) Submitted.
41. Mazur, S. J., and Grossman, L. (1991) *Biochemistry 30*, 4432−43.
42. Myles, G. M., Hearst, J. E., and Sancar, A. (1991) *Biochemistry 30*, 3824−34.
43. Machius, M., Henry, L., Palnitkar, M., and Deisenhofer, J. (1999) *Proc. Natl. Acad. Sci. U.S.A. 96*, 11717−22.
44. Theis, K., Chen, P. J., Skorvaga, M., Van Houten, B., and Kisker, C. (1999) *EMBO J. 18*, 6899−907.
45. Moolenaar, G. F., Visse, R., Ortiz-Buysse, M., Goosen, N., and van de Putte, P. (1994) *J. Mol. Biol. 240*, 294−307.
46. Ya, N.-Q., Smirnov, S., Cosman, M., Bhanot, S., Ibanez, V., and Geacintov, N. E. (1993) In *Structural Biology: The State of the Art. Proceedings of the 8th Conversataion* (Sarma, R. H., and Sarma, M. H., Eds.) Vol. 2, pp 349−66, Adenine Press, Schenectady, NY.
47. Geacintov, N. E., Cosman, M., Hingerty, B. E., Amin, S., Broyde, S., and Patel, D. J. (1997) *Chem. Res. Toxicol. 10*, 111−46.
48. Evans, E., Fellows, J., Coffer, A., and Wood, R. D. (1997) *EMBO J. 16*, 625−38.
49. Mu, D., Wakasugi, M., Hsu, D. S., and Sancar, A. (1997) *J. Biol. Chem. 272*, 28971−79.

BI001504C